EXIT-chart Aided Joint Source-Coding, Channel-Coding and Modulation Design for Two-Way Relaying

A. J. Aljohani, S. X. Ng, R. G. Maunder and L. Hanzo

School of Electronics and Computer Science, University of Southampton, SO17 1BJ, United Kingdom.

Tel: +44-23-8059 3125, Fax: +44-23-8059 4508

Email: {ajra1c09,sxn,rm,lh}@ecs.soton.ac.uk, http://www-mobile.ecs.soton.ac.uk

Abstract— **In this contribution, we have proposed and investigated an attractive Joint Source-coding, Channel-coding and Modulation (JSCM) scheme for a two-way relaying system. We commence by quantifying the achievable capacity of the corresponding two-way relay channel, before proposing low-complexity source coding schemes for concatenation with bandwidth-and power-efficient coded modulation schemes. Extrinsic Information Transfer (EXIT) charts is used to investigate the decoding convergence of the joint source and channel decoder as well as for the overall system design. The quality of the decoded source signals is quantified using the Bit-Error Ratio (BER) metric. It is found that the two-way relay based JSCM scheme is capable of attaining a combined coding and relaying gain of 5.7 dB over the conventional non-cooperative JSCM scheme, when communicating over uncorrelated Rayleigh fading channels in an outdoor environment.**

Index Terms— **Two-way relay, Turbo Trellis Coded Modulation, iterative decoding, power sharing, source coding, channel coding.**

I. INTRODUCTION

Two-way or bi-directional relay systems have drawn increasing research attention, since they overcome the potential spectral efficiency loss of one-way relaying scheme [1]–[3]. The system supports two user-terminals acting as Source Nodes (SNs) that want to exchange their information with the aid of a Relay Node (RN). In the conventional one-way relay schemes, four time slots are required for accomplishing a full information exchange. By contrast, two-way relaying requires only two time slots for duplex information exchange. The two-way relay channel capacity achieved for Gaussian-input signals and for a quasi-static fading profile has been investigated in [4], [5] and in the references therein. Recently, a Turbo Trellis Coded Modulation (TTCM) [6] aided two-way relaying scheme based on a power-sharing technique was investigated in [7],

where a significant Bit Error Ratio (BER) improvement was achieved. However, the capacity of the power-sharing based two-way relay channel has not been quantified.

Variable Length Codes (VLCs) constitute a family of low-complexity lossless source compression schemes. Numerous trellis-based VLC decoding techniques have been proposed for exploiting the residual redundancy inherent in VLCs. More specifically, an attractive joint source/channel coding scheme based on the bit-based trellis structure of [8] was proposed in [9], while a range of near-capacity Joint Source-coding, Channel-coding and Modulation (JSCM) schemes were investigated in [10], [11]. Recently, the JSCM schemes of [10] was extended to a one-way cooperative communication system in [12], where a significant amount of coding and

relaying gain was attained at the cost of halving the throughput due to the employment of a half-duplex relay node.

Extrinsic Information Transfer (EXIT) charts [13], [14] have been used for designing near-capacity channel codes [12], [15], [16]. We employ EXIT chart for the following three reasons. Firstly, it is used for investigating the minimum required Signal-to-Noise Ratio (SNR) in both the Phase-I and Phase-II links in order to derive the optimum power allocation. Secondly, the EXIT chart has been invoked to find the optimum number of iterations between the TTCM and VLC decoders with a trade-off in terms of complexity and performance gain. This can be achieved through creating of an open EXIT chart tunnel [17], [18] for achieving decoding convergence to an infinitesimal low BER at a channel SNR close to the channel's capacity bound. Thirdly, it is used to investigate the decoding convergence between the joint TTCM-VLC decoder and the Multi-User Detector (MUD). In a nutshell EXIT-chart allows us to entirely move away from the classic design principles relaying on finding codes with a large minimum distance. Instead a large design-space may be readily explored by simply finding the components, which allow the system to reach the corner point of perfect convergence to a vanishingly low BER.

Against this background, we aim for designing an energy-efficient JSCM scheme that can simultaneously exploit the capacity of the two-way relay channel and the residual redundancy of the source signals. More specifically, the proposed JSCM scheme is designed with the aid of EXIT charts for attaining a high transmission energy-efficiency with the aid of iterative decoding. Further transmission energy savings may be attained with the aid our proposed power-allocation technique. Then, low-complexity source coding schemes are invoked for attaining processing energy-efficiency by exploiting the source signals' residual redundancy and by using VLCs. Iterative detection exchanging extrinsic information between the MUD detectors, TTCM decoder and VLC decoder invoked which is jointly optimized using EXIT charts for achieving both transmission and processing energy-efficiencies. In other words, the capacity of the two-way relay channel and the redundancy of the source signals can be jointly exploited via extrinsic mutual information exchange between the MUD detectors and the JSCM (TTCM-VLC) decoder. The novel contributions can be summarized as follows:

1) *We quantify the achievable capacity of the two-way relaying scheme of [7];*
2) *The EXIT chart tool is used for determining the number of iterations between the TTCM and VLC decoders required, for achieving an early decoding convergence between the JSCM (TTCM-VLC) decoder and the MUD detectors during both transmission phases and for sharing the transmission power between the two source nodes and the relay node;*
3) *The single-user JSCM schemes of [10], [11] will be extended to a two-user based two-way relaying system.*
4) *Low-complexity source-coding schemes are proposed and investigated based on the transmission of images across the*

two-way relay channel.

The rest of the paper is organized as follows. Our system model is described in Section II, while the corresponding channel capacity is derived in Section III. The proposed scheme is designed and investigated in Section IV, while two low-complexity source-coding schemes are conceived and characterized in Section V. Finally, our conclusions are offered in Section VI.
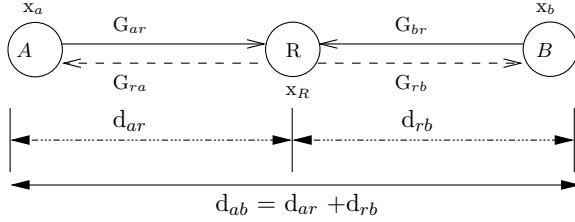
II. SYSTEM MODEL

Fig. 1: Schematic of a two-hop relay-aided system, where d_{ab} is the geographical distance between node a and node b.

The schematic of our proposed two-way relaying scheme is shown in Fig. 1, where both users A and B has a single antenna each. They exchange their information with the aid of a RN equipped with two antennas. The two users may also be treated as a single two-transmitter distributed *virtual* SN. The communication paths shown in Fig. 1 are subjected to both path-loss and uncorrelated Rayleigh fading. Assuming a pathloss exponent of three for an outdoor environment [19], the corresponding reduced-pathloss-induced geometrical gain experienced by the Source-to-Relay (SR) link and Relay-to-Destination (RD) link with respect to the Source-to-Destination(SD) link may be calculated, respectively, as [18], [20]:

$$G_{ar} = \left(\frac{d_{ab}}{d_{ar}}\right)^3 \quad ; \quad G_{rb} = \left(\frac{d_{ab}}{d_{rb}}\right)^3 , \tag{1}$$

where d_{ab} denotes the distance between node a and node b. Without loss of generality, we assume that the twin-antenna-assisted RN is located midway between the two SNs. Hence, we have $G_{ar} = G_{rb} = 8$, which corresponds to 9 dBs. If $P_{t,a}$ is the power transmitted from node a, the average receive SNR per-user per-receive antenna[1] at node b is given by [7]:

$$\text{SNR}_r = \frac{P_{t,a}\text{E}\{G_{ab}\}}{N_0} \cdot \frac{\sum_{b_i=1}^{N_b} \sum_{a_j=1}^{N_a} \text{E}\{|h_{b_i a_j}|^2\}\text{E}\{|x_{a_j}|^2\}}{N_b N_a}$$
$$= \frac{P_{t,a}G_{ab}}{N_0}, \tag{2}$$

where the number of antennas at node a and b is represented by N_a and N_b, respectively. Moreover, x_{a_j} is the symbol transmitted from the jth antenna of node a, $h_{b_i a_j}$ represents the channel coefficients for the link between the jth antenna of node a and the ith antenna of node b, while the expected values are given by $\text{E}\{|h_{b_i a_j}|^2\} = 1$ and $\text{E}\{|x_{a_j}|^2\} = 1$. It is convenient for our discussions to define the term referred to as transmit SNR[2] as the the ratio of the power transmitted from node a to the noise power experienced at the receiver of node

---

[1]The terminology of per-user, per-receive antenna was introduced in order to conduct a fair comparison among the different scenarios considered and to emphasize the fact that these results may be applicable to other relaying schemes.

[2]However, the concept of transmit SNR [20] is unconventional, as it relates quantities to each other at two physically different locations, namely the transmit power to the noise power at the receiver.

b as $\gamma_T = P_{t,a}/N_0$. Thus, we have $\gamma_R = \gamma_T G_{ab}$, which can be expressed in decibel as:

$$\Gamma_R = \Gamma_T + 10\log_{10}(G_{ab}) \text{ [dB] }, \tag{3}$$

where we have $\Gamma_R = 10\log_{10}(\gamma_R)$ and $\Gamma_T = 10\log_{10}(\gamma_T)$. Hence the receive SNR is larger than the transmit SNR when the geometrical gain [18], [20], which is normalized with respect to the SD link, is higher than unity. In our case, the average receive SNR is always 9 dB above the average transmit SNR according to Eq. (3) because we have $G_{ar} = G_{rb} = 8$.

The Phase-I transmission from the $L = 2$ SNs to the $P = 2$ antenna based RN may be viewed as a Space-Division Multiple Access (SDMA) [21] based scheme, where MUD techniques can be employed at the RN. The channel between the two users and the RN can be represented by an $(P \times L)$-dimensional channel matrix $\mathbf{H}$ and the received signal at the RN may be written as:

$$\mathbf{y} = \mathbf{Hx} + \mathbf{n}, \tag{4}$$

where the transmitted symbol $\mathbf{x} = [x_0, x_1, \cdots, x_{L-1}]^T$ is an $(L \times 1)$-dimensional vector, while the received signal $\mathbf{y} = [y_0, y_1, \cdots, y_{P-1}]^T$ is an $(P \times 1)$-dimensional vector and $\mathbf{n}$ represents the complex-valued $(P \times 1)$-dimensional AWGN vector having a variance of $N_0/2$ per dimension. We incorporated the reduced-pathloss-induced geometrical gain [22], [20] and the transmitted power factor in $\mathbf{H}$ of Eq. (4). Therefore the channel of the Phase-I link can be expressed as:

$$\mathbf{H} = \begin{bmatrix} \sqrt{G_{ar_1}}\sqrt{P_{t,a}}h_{ar_1} & \sqrt{G_{br_1}}\sqrt{P_{t,b}}h_{br_1} \\ \sqrt{G_{ar_2}}\sqrt{P_{t,a}}h_{ar_2} & \sqrt{G_{br_2}}\sqrt{P_{t,b}}h_{br_2} \end{bmatrix}, \tag{5}$$

where the ith receive antenna of the RN is denoted by the subscript r_i, while $P_{t,a}$ represents the power transmitted from user A and h_{ar_i} signifies the Channel impulse response (CIR) coefficient between user A and antenna r_i. The reduced-pathloss-induced geometrical gains between user A (user B) and antenna r_i is denoted by G_{ar_i} (G_{br_i}). The RN invokes three types of SDMA-based MUDs, namely the optimum but relatively complex Maximum Likelihood (ML), Minimum Mean-Square Error-assisted Interference Cancellation (MMSE-IC) and the sub-optimum Zero Forcing (ZF) MUDs.

The Phase-II transmission is shown in the lower part of Fig. 2. The RN concatenates the two decoded N-bitsequences into a $2N$-bit sequence, yielding $\hat{b}_3 = [\hat{b}_1 \ \hat{b}_2]$. Then, the combined sequence $\hat{b}_3$ is encoded by a TTCM encoder before it is broadcast from the RN back to the two users. The Phase-II transmission channel may be viewed as in an SDMA system using two transmit antennas and one receive antenna. Each user then detects and decodes the signal in a similar manner to that used at the RN. In our simulations we only consider the ML MUD in the challenging rank-deficient Phase-II link, since the number of receiver antennas should be at least equal to the number of transmit antennas when using MMSE and ZF schemes. In order to further improve the attainable performance of the MMSE MUD, interference cancellation (MMSE-IC) [7] has been invoked for iteratively eliminating the inter-user interference. Further details on SDMA detection can be found from [7], [23].

The proposed scheme can be extended to support an arbitrary number of users having in mind the following limitations:

- Higher hardware complexity at the RN:
  If the number of receive antennas at the RN is equal to or higher than the number of users, then low complexity MMSE and ZF MUDs can be implemented at the RN. During the Phase-II transmission, each RN's transmit antenna can be used for carrying independent user signals by forming an SDMA
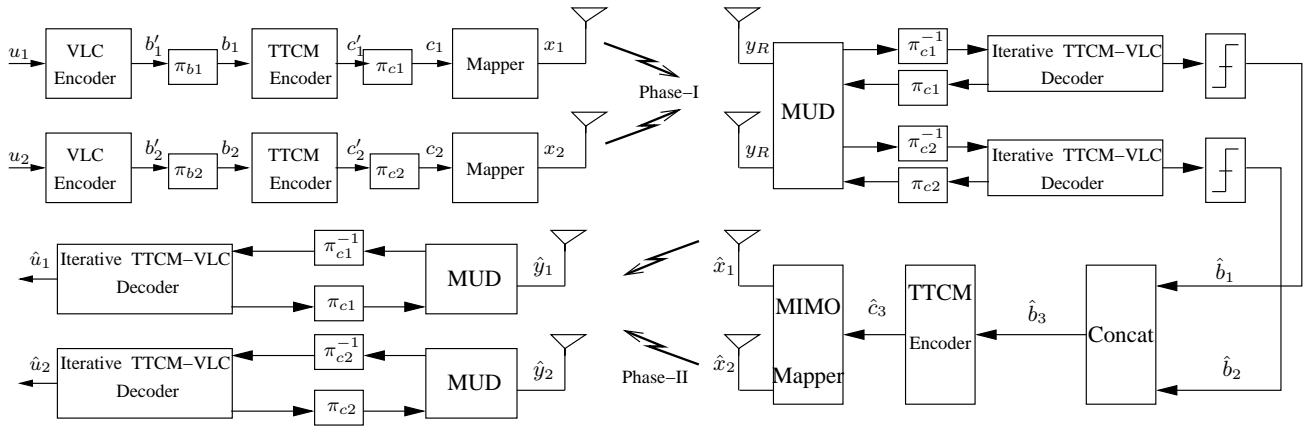
Fig. 2: The schematic of the joint TTCM-VLC-aided SDMA assisted two-way relay system.

system. However, this leads to a significant increase in the RN's hardware complexity.

- Higher detection complexity and lower bandwidth efficiency: If the number of receive antennas at the RN is less than the number of users, then a high complexity ML MUD has to be employed at the RN, which leads to a higher detection complexity at the RN. Furthermore, SDMA cannot be used during the Phase-II transmission. Hence, more timeslots (TDMA) or frequency bands (CDMA/FDMA) are required, which leads to a lower bandwidth efficiency during the Phase-II transmission.

A. Source Coding Scheme

The TTCM assisted VLC (TTCM-VLC) scheme of [11] is invoked in our two-way relay system, since the TTCM-VLC arrangement was found to be the best one from a range of other coded modulation assisted VLC schemes in [11]. The block diagram of the TTCM-VLC-aided SDMA based two-way relaying (TTCM-VLC-2Way) scheme is shown in Fig. 2, where each user employs a serial-concatenated Reversible VLC (RVLC)[3] and a TTCM scheme. Note that a bit-based interleaver is used between each pair of the VLC and TTCM encoders. We employed the same source as that used in [10]–[12] so that all results are comparable. More specifically, we invoked the RVLC of [25], where the source symbols are $u = \{0, 1, 2, 3, 4\}$ and the corresponding probabilities of occurrence are given by $P(u) = \{0.33, 0.30, 0.18, 0.10, 0.09\}$. The legitimate VLC codewords are $C = \{00, 11, 010, 101, 0110\}$ and the associated entropy is $L_s = 2.1391$ bits/symbol, while the calculated average codeword length is $L_{vlc} = 2.46$ bits/VLC symbol. Hence, the source coding efficiency is given by $R_{vlc} = L_s/L_{vlc} = 0.87$.

The interleaved VLC-encoded bits, b_1 and b_2 are encoded with the aid of an 8PSK based rate-$2/3$ TTCM encoder. Memory-three TCM constituent codes having an octally represented generator polynomial of $[11 \ 2 \ 4 \ 10]_8$ are employed. The two TTCM-VLC codewords c_1 and c_2 are then fed into a virtual MIMO mapper after being interleaved by the symbol interleaver π_{c1} (or π_{c2}), as shown in Fig. 2. The estimated information sequences $\widehat{b}_1$ and $\widehat{b}_2$ are detected by exchanging *extrinsic* information between the MUD and the iterative joint TTCM-VLC decoders, as shown in the upper part of Fig. 2.

The overall throughput of this two-way relaying scheme may be

[3]Our design is applicable to any VLCs. However, the reversible VLCs are particularly suitable for iterative detection, because they have a minimum free distance of 2, as detailed in [17] and [24]. This allows the iterative detector to approach a vanishingly low BER at low SNR.

formulated as:

$$\eta = \frac{LN_i}{N_s + N_r}, \quad (6)$$

where N_i is the number of information bits transmitted within a duration of $(N_s + N_r)$ symbol periods and L denotes the number of users. Furthermore, N_s is the number of modulated symbols per frame transmitted from the SNs during the first time slot and N_r is the number of modulated symbols per frame transmitted from the RN during the second time slot. We have $N_s = N_r$ and we do not apply trellis termination for the TTCM encoder. Therefore, we have $N_i = mR_{vlc}N_s \approx 1.74N_s$, since we have $m = 2$ information bits per 8PSK symbol after the rate-$2/3$ TTCM encoder. Hence, the overall throughput of our system is $\eta \approx 1.74$ bits per symbol (bps).
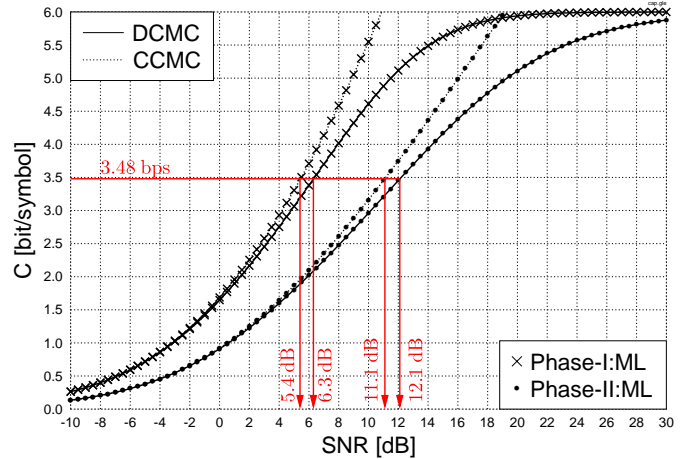
III. TWO-WAY RELAY CHANNEL CAPACITY

Fig. 3: DCMC and CCMC capacity curves of the 8-PSK based non-relay scheme for both phases, where the curves were computed based on [26], [27].

The Continuous-Input-Continuous-Output Memoryless Channel (CCMC) and the Discrete-Input-Continuous-Output Memoryless Channel (DCMC) [26], [27] capacities of the (2×2) Phase-I link and the (2×1) Phase-II links are shown in Fig. 3. Although the overall throughput per timeslot is given by 1.74 bps, the throughput during each timeslot is 3.48 bps. Based on the DCMC (CCMC) capacity curves of Fig. 3, the corresponding SNR_r required for Phase-I and Phase-II at a throughput of $\eta = 3.48$ bps are 6.3 dB (5.4 dB) and 12.1 dB (11.1 dB), respectively.

According to the max-flow min-cut theorem [28], the information flow from the source to the destination is limited by the specific link having the minimum capacity. Since the capacity of the (2×2) Phase-I link is higher than that of the (2×1) Phase-II link, the capacity of the two-way relay channel is limited by the Phase-II link if the power- and time-allocation is not optimized. More specifically, the capacity of the two-way relay channel may be formulated as:

$$C_{2\text{way}}(\overline{\Gamma}_R) = \max_{\text{Power \& Time}} \min\left[\lambda_I C_I(\Gamma_{R,s}), \lambda_{II} C_{II}(\Gamma_{R,r})\right] , \quad (7)$$

which is maximized by appropriate dynamic transmission power- and/or time-allocation, where λ_I and λ_{II} are the fraction of transmission duration for Phase-I and Phase-II, respectively. From Eq. (7), when λ_I (λ_{II}) is low, the transmission duration of the SN (RN) is short. Thus, the coding rate of a fixed modulation scheme and/or the modulation levels used in an adaptive coding and modulation scheme has to be increased in order to achieve an increased throughput. Naturally, the receiver has to be aware of the detection time, coding rate and/or modulation mode.

Furthermore, $C_I(\Gamma_{R,s})$ is the Phase-I link capacity at a receive SNR of $\Gamma_{R,s} = 10\log_{10}(\gamma_{R,s})$ and $C_{II}(\Gamma_{R,r})$ is the Phase-II link capacity, when the receive SNR of that link is given by $\Gamma_{R,r} = 10\log_{10}(\gamma_{R,r})$. The average receive SNR, $\overline{\Gamma}_R = 10\log_{10}(\overline{\gamma}_R)$, of the two-way relay scheme is given by:

$$\overline{\Gamma}_R = 10\log_{10}\left(\frac{10^{\frac{\Gamma_{R,s}}{10}} + 10^{\frac{\Gamma_{R,r}}{10}}}{2}\right) . \quad (8)$$

In our system, we have $\lambda_I = \lambda_{II} = 0.5$ [4], because the transmission periods for both phases are identical, i.e. $N_s = N_r$. It may be seen from Eq. (7) that $C_{2\text{way}}(\overline{\Gamma}_R)$ is maximized for a given $\overline{\Gamma}_R$, when $C_I(\Gamma_{R,s}) = C_{II}(\Gamma_{R,r})$ if $\lambda_I = \lambda_{II}$. Hence, the two-way relay channel capacity may be expressed as:

$$C_{2\text{way}}(\overline{\Gamma}_R) = 0.5 \, C_I(\Gamma_{R,s}) = 0.5 \, C_{II}(\Gamma_{R,r}) , \quad (9)$$

when $\lambda_I = \lambda_{II}$.

A. Quasi-Static Rayleigh Fading Channel

For quasi-static fading channels, the CCMC-based two-way relay channel capacity is achieved, when the CCMC capacity of Phase-I, $C_I^*(\Gamma_{R,s})$, equals that of Phase-II, $C_{II}^*(\Gamma_{R,r})$, as follows:

$$C_I^*(\Gamma_{R,s}) = C_{II}^*(\Gamma_{R,r}) , \quad (10)$$

$$\log_2\left(\prod_{k=1}^{2}(1 + \gamma_{R,k})\right) = \log_2(1 + \gamma_{R,0}) , \quad (11)$$

where $\gamma_{R,k} = \gamma_{T,s}\lambda_k/N_t$ is the receive SNR in the kth subchannel of the (2×2) MIMO channel, $\sqrt{\lambda_k}$ is the kth singular value of the (2×2) MIMO channel in Eq. (5) and $\gamma_{T,s}$ is the transmit SNR of each user in the virtual SN equipped with $N_t = 2$ antennas. Similarly, $\gamma_{R,0} = \gamma_{T,r}\lambda_0/N_t$ is the receive SNR in the first (and only) subchannel of the (2×1) channel, which has a singular value of $\sqrt{\lambda_0}$, while $\gamma_{T,r}$ is the transmit SNR of the RN, which has $N_t = 2$

[4]It is not necessary for the two phases to have an equal duration for achieving an improved capacity, hence the time-resource-allocation techniques of [29] can also be invoked. In contrast to the time-resource-allocation techniques, the proposed PS method does not require any overhead or side-information for informing the receiver of the transmission power used. However, the time-resource-allocation technique relies on side-information for conveying the coding rate used and the modulation scheme employed to the receiver.

antennas. At a given transmit SNR of $\gamma_{T,s}$ at the SN, we can derive the optimal transmit SNR $\gamma_{T,r}$ at the RN based on Eq. (11) as:

$$\gamma_{T,r} = \frac{(1 + \lambda_1\gamma_{T,s}/2)(1 + \lambda_2\gamma_{T,s}/2) - 1}{\lambda_0/2} . \quad (12)$$

The corresponding optimal average transmit SNR may be formulated as:

$$\overline{\gamma}_T = \frac{\gamma_{T,s} + \gamma_{T,r}}{2} \quad (13)$$

$$= \frac{1}{\lambda_0}\left(\lambda_1\lambda_2\left(\frac{\gamma_{T,s}}{2}\right)^2 + (\lambda_0 + \lambda_1 + \lambda_2)\frac{\gamma_{T,s}}{2}\right) . \quad (14)$$

Hence, we can determine the optimal transmit SNR of the two-way relaying scheme for quasi-static fading channel, once the singular value of the Phase-I and Phase-II channels are determined.

B. Uncorrelated Rayleigh Fading Channel

However, the optimal transmit SNR of the two-way relaying system cannot be determined based on Eq. (14), when communicating over uncorrelated Rayleigh fading channels. More specifically, we can express the ergodic CCMC capacities of the Phase-I and Phase-II transmissions, as functions of their corresponding receive SNRs as:

$$C_I' = F_I(\Gamma_{R,s}) \;\; ; \;\; C_{II}' = F_{II}(\Gamma_{R,r}) , \quad (15)$$

which represent the CCMC capacity curves shown in Fig. 3. The corresponding receive SNR required for achieving a given target throughput can then be inferred from the capacity curves. Explicitly, the receive SNR required for achieving a throughput of 3.48 bps may be expressed as:

$$\Gamma_{R,s} = F_I^{-1}(C_I' = 3.48) = 5.4 \text{ dB} , \quad (16)$$

$$\Gamma_{R,r} = F_{II}^{-1}(C_{II}' = 3.48) = 11.1 \text{ dB} . \quad (17)$$

When the RN is located midway between the two SNs ($G_{rb} = G_{ar}$), the difference in terms of transmit SNR can be expressed as:

$$\begin{aligned}
\Gamma_{R,\Delta} &= \Gamma_{R,r} - \Gamma_{R,s} \\
&= (\Gamma_T + 10\log_{10}(G_{rb})) - (\Gamma_T + 10\log_{10}(G_{ar})), \\
&= \Gamma_{T,r} - \Gamma_{T,s} \text{ [dB]} = \Gamma_{T,\Delta} , \quad (18)
\end{aligned}$$

where $\Gamma_{R,\Delta} = 10\log_{10}(\gamma_{R,\Delta})$, $\Gamma_{T,\Delta} = 10\log_{10}(\gamma_{T,\Delta})$ and we have $\Gamma_{T,\Delta} = \Gamma_{R,\Delta} = 11.1 - 5.4 = 5.7$ dB in our CCMC case. Hence, the transmit SNR difference in the non-logarithmic domain is given by:

$$\gamma_{T,\Delta} = \frac{\gamma_{T,r}}{\gamma_{T,s}} . \quad (19)$$

When using Eq. (13) and Eq. (19), the new transmit SNR of the SN may be formulated as:

$$\gamma_{T,s} = \frac{2\overline{\gamma}_T}{1 + \gamma_{T,\Delta}}. \quad (20)$$

Similarly, the transmit SNR of the RN is given by:

$$\gamma_{T,r} = \frac{2\overline{\gamma}_T\gamma_{T,\Delta}}{1 + \gamma_{T,\Delta}}. \quad (21)$$

Hence, at a given average transmit SNR budget of $\overline{\gamma}_T$, we can allocate the appropriate transmit SNR for the SN and for the RN based on Eq. (20) and Eq. (21), respectively, once the transmit SNR difference $\gamma_{T,\Delta}$ was computed from the CCMC capacity curves. We refer to this transmit SNR computation as the Power Sharing (PS) technique[5]. The same procedure may be repeated for computing the corresponding transmit SNRs in the DCMC scenario.

[5]The PS technique based on Eq. (20) and Eq. (21) was first proposed in [7] based on simulation results. However, we found that it is also applicable, when aiming for achieving the two-way relay channel's capacity.
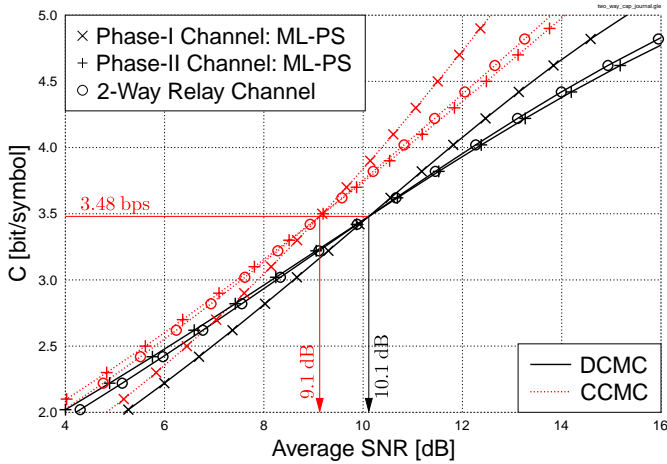
Fig. 4: The capacity versus average receive SNR curves of the Phase-I and Phase-II channels as well as that of the two-way relay channel.

Fig. 4 shows the capacity curves of the Phase-I and Phase-II channels, when aiming for achieving a target throughput of 3.48 bps. It may be seen from Fig. 4 that the CCMC (or DCMC) capacity curves of both Phase-I and Phase-II overlap at a throughput of 3.48 bps, when the average receive SNR is 9.1 dB (or 10.1 dB). By computing the SNR differences for different throughput values based on the capacity curves of Fig. 3, we arrive at the CCMC (and the DCMC) capacity curves of the two-way relay channel, as shown in Fig. 4 according to:

$$C'_{2\text{way}}(\overline{\Gamma}_R) = 0.5 \, F_I \left(10 \log_{10} \left(\frac{2\overline{\gamma}_T}{1 + \gamma_{T,\Delta}} \right) \right), \quad (22)$$

$$= 0.5 \, F_{II} \left(10 \log_{10} \left(\frac{2\overline{\gamma}_T \gamma_{T,\Delta}}{1 + \gamma_{T,\Delta}} \right) \right). \quad (23)$$

Note that we did not consider the factor 0.5, when plotting the two-way relay channel's capacity curves in Fig. 4 for the sake of clearly illustrating the point, where they intersect with the corresponding Phase-I and Phase-II capacity curves at a throughput of 3.48 bps.

IV. DESIGN AND ANALYSIS

Based on the PS technique of Section III-B, the achievable rate of the TTCM-VLC-2Way scheme may be computed based on its Phase-I and Phase-II performances. Note that user B is the Destination Node (DN) of user A and vice versa. Firstly, we have to find the minimum required receive SNRs at the RN and DN, which ensure that both links are capable of achieving the required target reliability. These receive SNRs may be found either from the semi-analytical EXIT chart [12], [15], [16], by observing the SNR where an open EXIT-tunnel emerges, or from the simulation based (BER) curve. Our simulation parameters are summarised in Table I. Again, we consider a RN located at the mid-point between the SN and DN, where the corresponding reduced-pathloss-induced geometrical gains are given by $G_{ar} = G_{rb} = 8$. The non-binary EXIT chart technique of [30] is used for visualising the input/output mutual information transfer characteristics of the non-binary TTCM-VLC and MUD decoders. The EXIT chart of our TTCM-VLC-aided SDMA decoder recorded for the SR and RD links is displayed in Fig. 5. It can be seen from Fig. 5 that the "iteration = 4" inner iterations within the outer block constituted by the TTCM and VLC can facilitate an open EXIT chart channel, while relaying on a lower number of iterations would lead to a closed tunnel, which results in a residual BER. However, increasing the number of inner TTCM-VLC iterations to "iteration = 8" would only provide a marginal gain at the cost of doubling the decoding
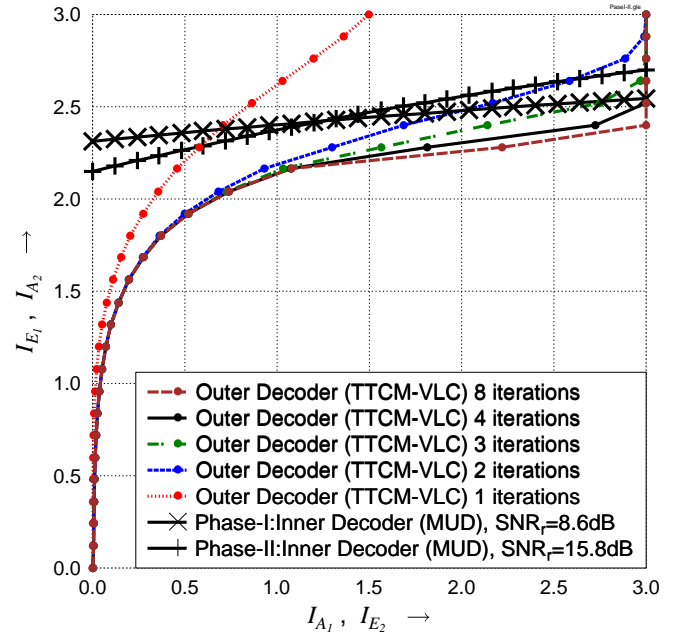

Fig. 5: The EXIT curves of the TTCM-VLC-aided MUD scheme for Phase-I Phase-II transmission, where the iteration of the outer curves is the inner iteration between the TTCM and VLC decoders. The TTCM decoder employs 4 internal iterations and the ML-based MUD is employed at both RN and DN.

TTCM-VLC Parameters	
VLC type	RVLC
CM type	TTCM
Modulation level	8-PSK
Number of transmitted symbol	10000 symbols per user
Decoding algorithm	Approximated Log-MAP [14]
TTCM decoder iteration number	4
TTCM-VLC decoder iteration number	4
TTCM-VLC-MUD iteration number	4
Source to Relay transmission:Phase-I	
Channel	Rayleigh Fading 2×2 MIMO
MUD Type	ML,MMSE-IC and ZF
G_{ar}	4 (6.02dB)
Relay to Destination transmission:Phase-II	
Channel	Rayleigh Fading 2×1 MIMO
MUD Type	ML
G_{rb}	4 (6.02dB)

TABLE I: System parameters.

complexity. As seen from Fig. 5, an open EXIT tunnel leading to the right-hand axis becomes available for the Phase-I transmission at $\text{SNR}_r = 8.6$ dB, which indicates that a decoding convergence to a vanishingly low BER is possible. Similarly, it is possible to attain an infinitesimally low BER at $\text{SNR}_r = 15.8$ dB for the Phase-II transmission. These EXIT chart predictions are confirmed by our simulation results shown in Fig. 6, where we have BER $\leq 10^{-6}$ at these SNR values. Note that since the open area of the EXIT chart tunnels is relatively wide, the Phase-I and Phase-II links operate at a distance of about 3 dB away from the corresponding DCMC capacities [6], as illustrated in Fig. 6.The various combinations considered were denoted by the legends: "4i 4o", "1i 4o" and "4i

[6] It is possible to further minimize the gap with regard to capacity by using irregular code designs [17], [18] at the cost of a higher decoding complexity, and a high interleaver length, i.e. latency, which precludes inter-active lip-synchronised video communication.

1o", where (o) represents the number of outer iterations between the TTCM-VLC decoder of Fig. 2 and the MUD, while (i) denotes the inner iterations between the VLC and TTCM decoders. Observe in

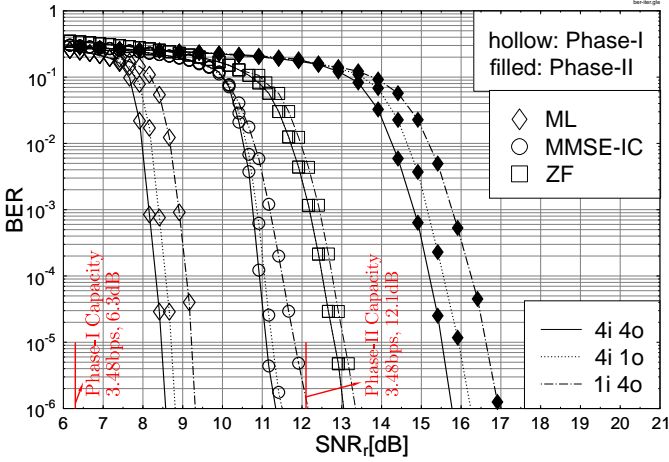$4.02 - 1.1 = 2.92$ dB away from the DCMC capacity bound.

Fig. 6: BER versus transmitted SNR per-user per-receiver antenna performance of TTCM-VLC-aided SDMA scheme with ML, MMSE-IC and ZF detections in the both source to relay and relay to destination links. The TTCM decoder invokes 4 inner iterations.

Fig. 6 that at a BER of 10^{-6} a marked improvement is exhibited for the ML-based scheme, when the number of inner iterations is increased. A slight improvement can be seen in Fig. 6 for the MMSE-based scheme, when the number of outer iterations is increased from one to four. The PS method is used for determining the optimum transmission power levels at each node required for exactly matching the capacity limit, as detailed in Section III-B. However, when practical coding and modulation schemes are employed, we have to find a more practical power allocation scheme based on the EXIT charts and simulation curves. More explicitly, the corresponding EXIT chart based and simulation-based SNR difference is given by $\Gamma_{T,\Delta} = \Gamma_{R,\Delta} = 15.8 - 8.6 = 7.2$ dB, as opposed to the DCMC-based SNR difference of $12.1 - 6.3 = 5.8$ dB. We employ the PS technique based on Eq. (20) and Eq. (21) using the SNR difference of 7.2 dB for our TTCM-VLC-2Way system. We will use the single-user non-cooperative TTCM-VLC scheme of [11] as our benchmark, whose throughput is 1.74 bps when 8PSK is employed. Our TTCM-VLC-2Way schemes have the same throughput and also enjoy a geometrical gain of 9 dB, due to employing a RN. Hence, the corresponding transmit SNR at the two-way relay based DCMC capacity of $3.84/2 = 1.74$ bps, is given by $\text{SNR}_t = \text{SNR}_r - 9 = 1.1$ dB, where the $\text{SNR}_r = 10.1$ dB limit is illustrated in Fig. 4. The BER versus SNR_t performance of 8PSK based TTCM-VLC and TTCM-VLC-2Way schemes, when communicating over uncorrelated Rayleigh fading channels, are depicted in Fig. 7. The three different MUD techniques, namely the above-mentioned ML, MMSE-IC and ZF were invoked in the RN during the first time slot, while only the ML was used at the DN during the second time period. It can be seen from Fig. 7 that without using the PS technique, the ML-based TTCM-VLC-2Way (denoted by a square marker with a dotted line) scheme will outperformed the TTCM-VLC scheme, but only by 3.3 dB at a BER of 10^{-6}. By contrast, a further 2.4 dB SNR gain can be attained by the ML-based TTCM-VLC-2Way scheme, when the PS technique is invoked. The performance of the "MMSE-IC-PS" and the "ZF-PS" based TTCM-VLC-2Way schemes was 0.65 dB and 1.24 dB poorer than that of the "ML-PS" based TTCM-VLC-2Way scheme at a BER of 10^{-6}. At a BER of 10^{-6} the proposed ML-PS based TTCM-VLC-2Way scheme is approximately
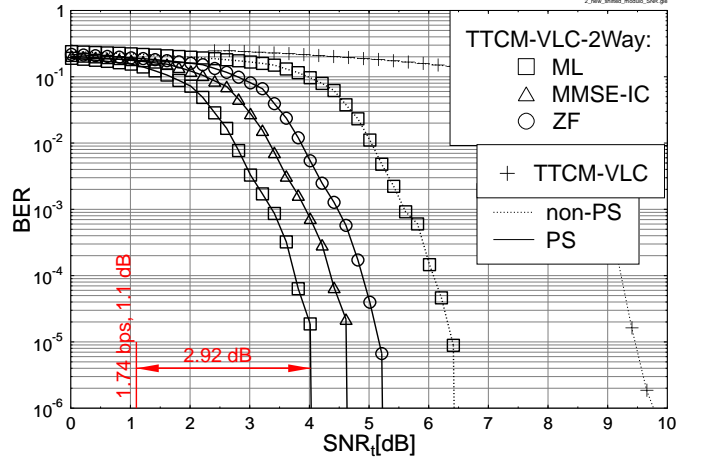

Fig. 7: BER versus SNR_t performance of 8PSK based TTCM-VLC as well as ML, MMSE-IC and ZF based TTCM-VLC-2Way schemes when communicating over uncorrelated Rayleigh fading channels. All schemes has an identical throughput of 1.74 bps.
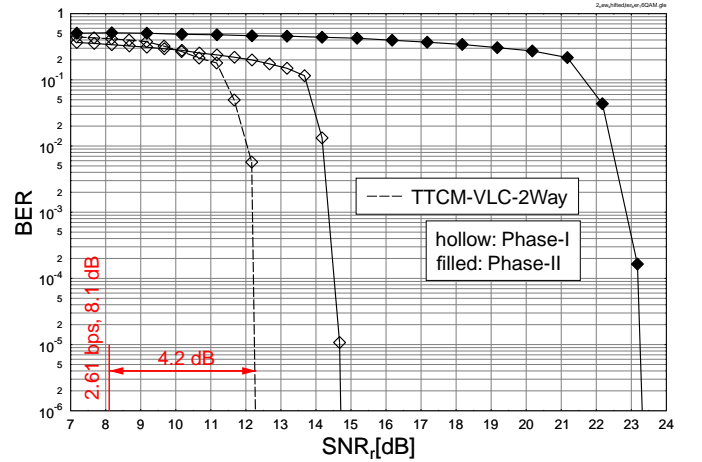

Fig. 8: BER versus transmitted SNR per-user per-receiver antenna performance of TTCM-VLC- aided SDMA- based **16QAM** scheme in the both source to relay and relay to destination links, as well as the two-way relaying-aided scheme. Note that, **ML** is used in both Relay and Destination nodes.

Furthermore, we have extended the above 8PSK-based system to a 16QAM-based scheme and investigated the corresponding performance in Fig. 8. The 16QAM-based scheme exhibits similar performance trends to those of the 8PSK-based scheme. Hence, our design is applicable to other modulation schemes. Note that we have used the 8PSK-based scheme for the rest of the study. In our future work, we will extend our two-way relaying scheme for supporting more users with the aid of advanced algorithms employed at the RN and DNs. In conclusion, our proposed mobile multimedia system provides a beneficial source compression with the aid of an RVLC, an improved error resilience by TTCM, as well as attaining both relaying and iterative gains. Let us now investigate the performance of the proposed TTCM-VLC-2Way schemes based on image transmissions in Section V.

V. Low-Complexity Source Coding

We proposed two low-complexity methods for image compression, by representing the image's pixels with the aid of a reduced number

of codewords. This would lead to a significant reduction in the complexity of the VLC decoding by decreasing the number of trellis-states. In our simulations, one of the users encodes the (256×256)-pixel Lena image, while the other user's signal is considered to be the interference. The most straightforward source encoding would be to map each pixel to a VLC source symbol, where the alphabet size is $2^8 = 256$, since each pixel is represented by 8 bits. However, this would incur a complex VLC trellis, which consists of 965 states, according to the bit-based trellis structure of [8]. The VLC decoding complexity would become excessive.
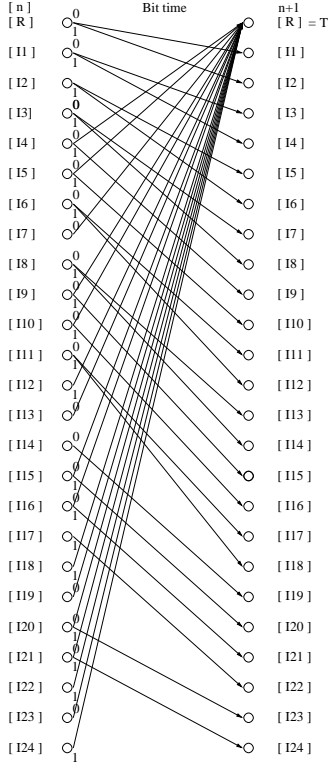
A. Source Coding Design

Fig. 9: Trellis diagram for M1 scheme.

In our first proposed method (M1), each 8 bits-per-pixel (b/p) symbol of the image is split into two 4 b/p symbols. This would reduce the number of possible symbols from $2^8 = 256$ to $2^4 = 16$, while the total number of source symbols is increased from $256 \times 256 = 65\ 536$ to $65\ 536 \times 2 = 131\ 072$. The number of VLC trellis states will be reduced dramatically from 965 to 25, as shown in Fig. 9. The trellis diagram between the bit time indices n and $n + 1$ is shown in Fig. 9, where there is a single root state corresponding to the root node R of the code tree[7] and a number of further states, that are labelled by the internal nodes $I1 \ldots I24$ of the code tree. All terminal nodes lead again to the root state $R = T$. This is a time-invariant bit-based trellis structure designed according to [8].

Our second method (M2) aims for further reducing the VLC decoding complexity by encoding the differences of the pixel values, rather than the actual pixel values. The flow-chart of Fig. 10 illustrates the encoding process of M2, where the current image pixel will be stored in the variable $\mathrm{Img}(x_i, y_j)$, while the prediction of the current

[7]The corresponding code tree is not shown due to the lack of space but the reader is referred to [8] for more details on the code tree structure.
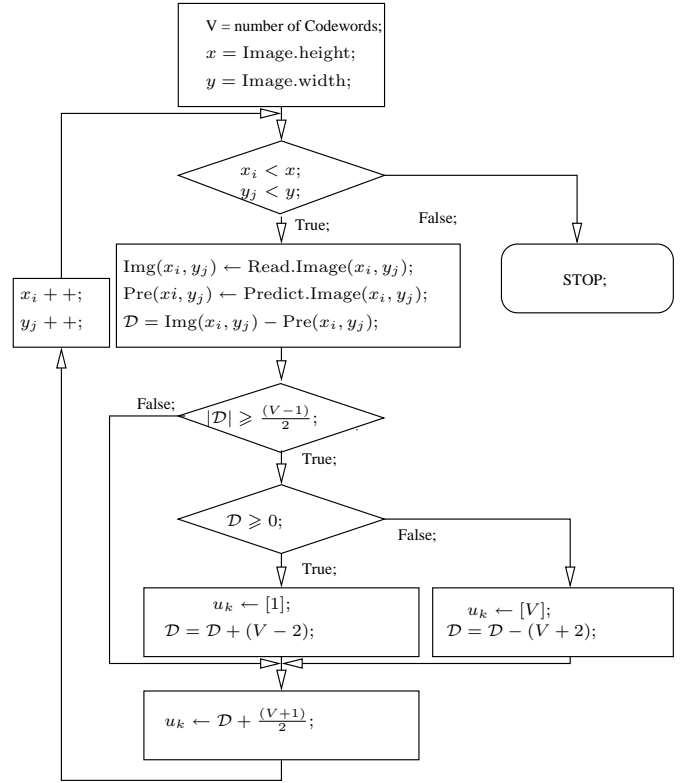
Fig. 10: The flow chart of the M2 encoder, where u_k will be feed into the VLC encoder as shown in Fig. 2.

pixel is computed based on the average value of the adjacent left pixel ($\mathrm{Img}(x_{i-1}, y_j)$) and adjacent top pixel ($\mathrm{Img}(x_i, y_{j-1})$) as follows:

$$\mathrm{Pre}(x_i, y_j) = 0.5\left[\mathrm{Img}(x_{i-1}, y_j) + \mathrm{Img}(x_i, y_{j-1})\right] . \quad (24)$$

The difference $\mathcal{D}$ of Fig. 10 between the two values, is then used for generating the 'pixel-difference' source symbols, as denoted by u_k in Fig. 10. The pixel-difference symbols u_k are encoded row-by-row from the top-left corner to the bottom-right corner. The complexity of the scheme and the number of codewords is controlled by the variable V, which should be an odd number. Note that in our simulations we have chosen $V = 9$ since it strikes a good tradeoff between the bit rate and the VLC decoding complexity. The number of states in the corresponding bit-based trellis is further reduced to 12, as illustrated in Fig. 11. Table II summarises the parameters of M1 and M2, where M1 has a smaller number of source symbols compared to M2, but it exhibits reduced source-symbol correlations, when the 8 b/p symbols are converted to 4 b/p symbols. As a result, the coding efficiency of M1 becomes lower and the total number of VLC bits required is $\lceil N_{ss} \times L_{vlc} \rceil = 604\ 164$. By contrast, M2 has a higher number of source symbols, but it efficiently reduces the average VLC codeword length by exploiting the inherent source correlations. As a result, the total number of VLC encoded bits in M2 is about 22% lower than that of M1. The transmit SNR per information bit for M1 and M2 can calculated as follows:

$$E_b/N_0[\mathrm{dB}] = \mathrm{SNR}_t[\mathrm{dB}] - 10\log_{10}(\eta) , \quad (25)$$

where we have $\eta = 1.7$ bps and $\eta = 1.78$ bps for M1 and M2 schemes, respectively, which have a difference of 0.08 bps. The Peak Signal-to-Noise Ratio (PSNR) for an $(m \times n)$-pixel monochrome
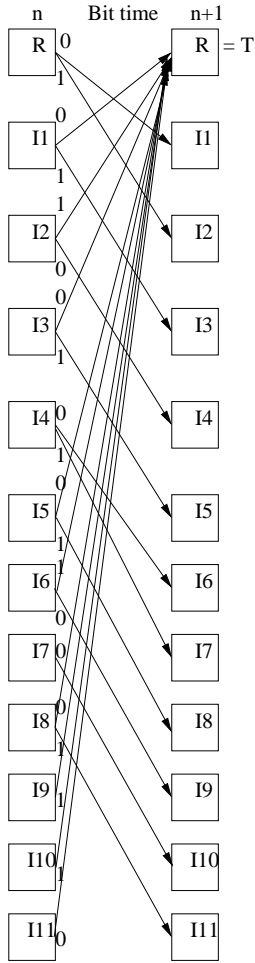
Fig. 11: Trellis diagram for M2 scheme.

(a) First iteration   (b) Second iteration   (c) Fourth iteration

Fig. 12: Subjective image quality of 8PSK-based TTCM-VLC for two-way relay system when communicating over uncorrelated Rayleigh fading channels. When $\mathbf{E_b/N_0 = 3.5}$ dB and $\mathbf{ML}$ is invoked in the RN and the number of outer iterations between the TTCM-VLC decoder of Fig. 2 and the MUD detector are (from left) one, two and four, respectively. The $\mathbf{M1}$-based source coding is used.

(a) First iteration   (b) Second iteration   (c) Fourth iteration
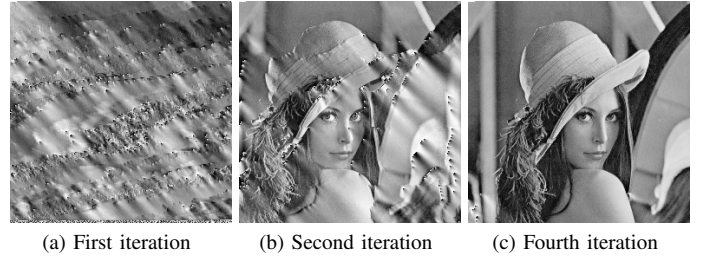
Fig. 13: Subjective image quality of 8PSK-based TTCM-VLC for two-way relay system when communicating over uncorrelated Rayleigh fading channels. When $\mathbf{E_b/N_0 = 3.5}$ dB and $\mathbf{ML}$ is invoked in the RN and the number of outer iterations between the TTCM-VLC decoder of Fig. 2 and the MUD detector are (from left) one, two and four, respectively. The $\mathbf{M2}$-based source coding is used.

image is given by [31]:

$$PSNR = 10 \log_{10} \left(\frac{I_{\max}^2}{\frac{1}{mn} \sum_{i=0}^{m-1} \sum_{j=0}^{n-1} \left| I_{i,j} - \hat{I}_{i,j} \right|^2} \right) , (26)$$

where we have $m = n = 255$ in our case, while $I_{i,j}$ is the original image pixel, $\hat{I}_{i,j}$ is the estimated image pixel and $I_{\max}^2$ is the maximum possible pixel value of the image. Following VLC and pixel-recovery, we have $I_{\max}^2 = 2^8 - 1 = 255$ for both M1 and M2. Since VLCs constitute lossless codes, when there is no error in the reconstructed pixels, we have $PSNR = \infty$. In order to avoid this, we normalize the PSNR values such that the maximum PSNR is given by $PSNR_{\max} = 10 \log_{10}(I_{\max}^2) = 48.13$ dB, where $1 \leq |I_{i,j} - \hat{I}_{i,j}| \leq 255$.

B. Performance Evaluation

The subjective image quality of the TTCM-VLC-2Way-ML scheme employing M1 and M2 is depicted in Fig. 12 and Fig. 13, respectively, while the corresponding PSNR versus E_b/N_0 performance are shown in Fig. 14.

As seen from Fig. 14, both the M1 and M2 based schemes are capable of achieving the asymptotic(error-free) PSNR at $E_b/N_0 = 3.5$ dB after the fourth iteration. Hence, the reconstructed images shown in Fig. 12c and Fig. 13c after the fourth iteration are perfect. However, the images shown in Fig. 12b and Fig. 13b at the second iteration are distorted in different ways. The M1-based image exhibits a few horizontal artefacts, while the M2-based image exhibits segments
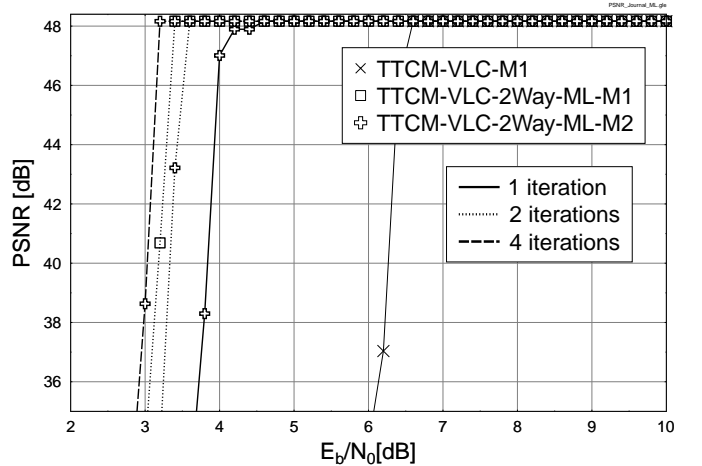

Fig. 14: The PSNR versus E_b/N_0 performance of 8PSK based TTCM-VLC scheme for two-way relay system when communicating over uncorrelated Rayleigh fading channel, where the $\mathbf{ML}$ was implemented in the RN and the iteration is the outer iterations between the TTCM-VLC decoder of Fig. 2 and the MUD detector.

moved to a different location. When aiming for a perfect transmission, the M2-based scheme only requires approximately 0.2 dB higher E_b/N_0 value than that of the M1-based scheme. Furthermore, M2 benefits from a lower complexity due to a lower number of VLC trellis states and a lower VLC bitrate, as summarised in Table II. Hence, the M2-based scheme offers a better tradeoff in terms of complexity and transmission bitrate. All TTCM-VLC-2Way schemes outperform the non-cooperative TTCM-VLC benchmark scheme.

	M1	M2
Number of Source Symbols, N_{ss}	131072	153060
Number of VLC codewords	16	9
Minimum codeword length	3	2
Maximum codeword length	7	6
Number of VLC trellis states	25	12
Average codeword length, L_{vlc}	4.6094	3.0932
VLC entropy, L_s	3.9189	2.7855
Coding efficiency, R_{vlc}	0.8502	0.8918
Total number of VLC bits	604,164	473,446
Final throughput, η [bps]	1.7	1.78

TABLE II: Comparison of parameters in M1 and M2.

VI. CONCLUSIONS

In this paper we have proposed a practical jointly optimized end-to-end source-coding, channel-coding and modulation scheme which was assisted by a two-way relaying scheme. This arrangement enables an exchange of two information frames between two users using only two, rather than four, cooperative time slots. EXIT chart was used to investigate the decoding convergence behaviour of the proposed scheme and for optimizing the overall system. It was shown in Fig. 7 that the proposed scheme outperformed the benchmark scheme dispensing with relaying by as much as 5.7 dB, when the appropriate power allocation strategy was invoked. We have also proposed two low-complexity source coding schemes for transmission over our two-way relaying system, where attractive PSNR and subjective image quality improvements were attained.

	Notations Table
BER	Bit Error Ratio
CCMC	Continuous-Input-Continuous-Output Memoryless Channel
CDMA	Code-Division Multiple Access
CIR	Channel Impulse Response
DCMC	Discrete-Input-Continuous-Output Memoryless Channel
EXIT	Extrinsic Information Transfer
FDMA	Frequency-Division Multiple Access
JSCM	Joint Source-coding, Channel-coding and Modulation
ML	Maximum Likelihood
MMSE	Minimum Mean-Square Error
MMSE-IC	Mean-Square Error-assisted Interference Cancellation
MUD	Multi-User Detection
PS	Power Sharing
PSNR	Peak Signal-to-Noise Ratio
RD	Relay-to-Destination
RN	Relay Node
RVLC	Reversible VLC
SD	Source-to-Destination
SDMA	Space-Division Multiple Access
SN	Source Node
SR	Source-to-Relay
TDMA	Time-Division Multiple Access
TTCM	Turbo Trellis Coded Modulation
VLCs	Variable Length Codes
ZF	Zero Forcing

TABLE III: Notations Table.

REFERENCES

[1] A. Sendonaris, E. Erkip and B. Aazhang, "User cooperation diversity part I: System description," *IEEE Trans. Commun.*, vol. 51, pp. 1927–1938, Nov. 2003.

[2] J. N. Laneman, D. N. C. Tse and G. W. Wornell, "Cooperative diversity in wireless networks: efficient protocols and outage behavior," *IEEE Trans. Inf. Theory*, vol. 50, pp. 3062–3080, Dec. 2004.

[3] K. J. Lee, H. J Sung, E. S. Park and I. K. Lee, "Joint optimization for one and two-way MIMO AF multiple-relay systems," *IEEE Trans. Wireless Commun.*, vol. 9, pp. 3671–3681, Dec. 2010.

[4] R. Vaze and R. W. Heath, "On the capacity and diversity-multiplexing tradeoff of the two-way relay channel," *IEEE Trans. Inf. Theory*, vol. 57, pp. 4219–4234, July 2011.

[5] A. Papadogiannis, A. G. Burr and M. Tao, "On the maximum achievable sum-rate of interfering two-way relay channels," *IEEE Commun. Lett.*, vol. 16, pp. 72–75, Jan. 2012.

[6] P. Robertson and T. Wörz, "Bandwidth-efficient turbo trellis-coded modulation using punctured component codes," *IEEE J. Sel. Areas Commun.*, vol. 16, pp. 206–218, Feb. 1998.

[7] W. Liang, S. X. Ng, L. Hanzo, "TTCM-aided SDMA-based two-way relaying," in *Proc. IEEE Vehicular Technology Conf.*, vol. 1, (San Francisco, USA), pp. 1–5, 5-8 Sept. 2011.

[8] V. B. Balakirsky, "Joint source-channel coding with variable length codes," in *IEEE International Symposium on Information Theory*, (Ulm, Germany), p. 419, 29 June-4 July 1997.

[9] R. Bauer, J. Hagenauer, "On variable length codes for iterative source/channel decoding," in *IEEE Data Compression Conf.*, (UT, USA), pp. 273–282, 27-29 March 2001.

[10] S. X. Ng, F. Guo, J. Wang, L-L. Yang and L. Hanzo, "Joint source-coding, channel-coding and modulation schemes for AWGN and Rayleigh fading channels," *Electron. Lett.*, vol. 39, pp. 1259–1261, Aug. 2003.

[11] S. X. Ng, F. Guo, J. Wang, L-L. Yang and L. Hanzo, "Jointly optimised iterative source-coding, channel-coding and modulation for transmission over wireless channels," in *Proc. IEEE Vehicular Technology Conf.*, (Milan, Italy), pp. 313–317, 17-19 May 2004.

[12] S. X. Ng, K. Zhu and L. Hanzo, "Distributed source-coding, channel-coding and modulation for cooperative communications," in *Proc. IEEE Vehicular Technology Conf.*, (Ottawa, Canada), pp. 1–5, Sept. 2010.

[13] S. ten Brink, "Convergence behaviour of iteratively decoded parallel concatenated codes," *IEEE Trans. Commun.*, vol. 49, pp. 1727–1737, Oct. 2001.

[14] L. Hanzo, T. H. Liew, B. L. Yeap, R. Y. S. Tee and S. X. Ng, *Turbo coding, turbo equalisation and space-time coding: EXIT-chart aided near-capacity designs for wireless channel*. New York, USA: John Wiley IEEE Press, 2011.

[15] X. Zuo, R. G. Maunder and L. Hanzo, "Design of fixed-point processing based ldpc codes using exit charts," in *Proc. IEEE Vehicular Technology Conf.*, (San Francisco, USA), pp. 3031–3035, 5-8 Sept. 2011.

[16] J. Wang and S.X. Ng and L-L. Yang and L. Hanzo, "Combined serially concatenated codes and mmse equalization: an exit chart aided perspective," in *Proc. IEEE Vehicular Technology Conf.*, pp. 3031–3035, Sept. 2006.

[17] R. G. Maunder, J. Wang, S. X. Ng and L. Hanzo, "On the performance and complexity of irregular variable length codes for near-capacity joint source and channel coding," *IEEE Trans. Wireless Commun.*, vol. 7, pp. 1338–1347, April 2008.

[18] L. Kong, S. X. Ng, R. G. Maunder and L. Hanzo, "Maximum-throughput irregular distributed space-time code for near-capacity cooperative communications," *IEEE Trans. Veh. Technol.*, vol. 59, pp. 1511–1517, March 2010.

[19] T. A. Fouad and M. M. Hira, "Joint optimization of physical layer parameters and routing in wireless mesh networks," in *The 9th IFIP Annual Mediterranean, Ad Hoc Networking Workshop (Med-Hoc-Net)*, pp. 1–8, June 2010.

[20] H, Ochiai, P. Mitran and V. Tarokh, "Design and analysis of collaborative diversity protocols for wireless sensor networks," in *Proceedings of IEEE VTC Fall*, (Los Angeles, USA), pp. 4645 – 4649, 26-29 September 2004.

[21] L. Hanzo, J. Akhtman, M. Jiang and L. Wang , *MIMO-OFDM for LTE, WIFI and WIMAX: coherent versus non-coherent and cooperative turbo-transceivers*. IEEE Press – John Wiley, 2011.

[22] S. X. Ng, Y. Li and L. Hanzo, "Distributed turbo trellis coded modulation for cooperative communications," in *Proceedings of International Conference on Communications (ICC)*, (Dresden, Germany), pp. 1–5, 14-18 June 2009.

[23] L. Hanzo, M. Münster, B. Choi, and T. Keller, *OFDM and MC-CDMA for Broadband Multi-user Communications, WLANs and Broadcasting*. John Wiley & Sons, May 2003.

[24] L. Hanzo, R. G. Maunder, J. Wang and L-L. Yang , *Near-capacity variable-length coding: regular and EXIT-chart-aided irregular designs*. Wiley-IEEE Press, 2010 .

[25] Y. Takishima, M. Wada and H. Murakami, "Reversible variable length codes," *IEEE Transactions on Communications*, vol. COM-43, no. 2/3/4, pp. 158–162, 1995.

[26] J. G. Proakis, *Digital Communications*. New York: Mc-Graw Hill International Editions, 3rd ed., 1995.

[27] S. X. Ng and L. Hanzo, "On the mimo channel capacity of multidimensional signal sets," *IEEE Trans. Veh. Technol.*, vol. 55, pp. 528–536, March 2006.

[28] R. Ahlswede, N. Cai, S.-Y. R. Li and R. W. Yeung, "Network information flow," *IEEE Transactions on Information Theory*, vol. 46, pp. 1204–1216, July 2000.

[29] L. Li and A. J. Goldsmith, "Capacity and optimal resource allocation for fading broadcast channels part ii: Outage capacity," *IEEE Trans. on Commun.*, vol. 4, pp. 1083–1102, March 2001.

[30] J. Kliewer, S. X. Ng and L. Hanzo, "Efficient computation of EXIT functions for non-binary iterative decoding," *IEEE Trans. Commun.*, vol. 54, pp. 2133–2136, December 2006.

[31] L. Hanzo, P. Cherriman, and J. Streit, *Wireless Video Communications: From Second to Third Generation Systems, WLANs and Beyond*. IEEE Press, 2001.

Abdulah Jeza Aljohani received the B.S. degree with honors in electronics a communication engineering from King Abdulaziz University (KAU), Jeddah, Saudi Arabia, in 2006. He received M.Sc. degree with distinction in wireless communication from University of Southampton, Southampton, U.K in 2009. He is currently working toward the Ph.D. degree in the Communications, Signal Processing and Control Group at the School of Electronics and Computer Science, University of Southampton, Southampton, UK. His current research interests include joint source/channel coding and distributed source coding.

Dr Soon Xin Ng (S'99-M'03-SM'08) received the B.Eng. degree (First class) in electronics engineering and the Ph.D. degree in wireless communications from the University of Southampton, Southampton, U.K., in 1999 and 2002, respectively. From 2003 to 2006, he was a postdoctoral research fellow working on collaborative European research projects known as SCOUT, NEWCOM and PHOENIX. Since August 2006, he has been a member of academic staff in the School of Electronics and Computer Science, University of Southampton. He is involved in the OPTIMIX and CONCERTO European projects as well as the IU-ATC and UC4G projects. He is currently a senior lecturer at the University of Southampton.

His research interests include adaptive coded modulation, coded modulation, channel coding, space-time coding, joint source and channel coding, iterative detection, OFDM, MIMO, cooperative communications, distributed coding, quantum error correction codes and joint wireless-and-optical-fiber communications. He has published over 150 papers and co-authored two John Wiley/IEEE Press books in this field. He is a Senior Member of the IEEE, a Chartered Engineer and a Fellow of the Higher Education Academy in the UK.

Robert G. Maunder (http://users.ecs.soton.ac.uk/rm) has studied with Electronics and Computer Science, University of Southampton, UK, since October 2000. He was awarded a first class honors BEng in Electronic Engineering in July 2003, as well as a PhD in Wireless Communications and a lectureship in December 2007. Rob's research interests include joint source/channel coding, iterative decoding, irregular coding and modulation techniques. He has published a number of IEEE papers in these areas.

Lajos Hanzo (http://www-mobile.ecs.soton.ac.uk) FREng, FIEEE, FIET, Fellow of EURASIP, DSc received his degree in electronics in 1976 and his doctorate in 1983. In 2009 he was awarded the honorary doctorate "Doctor Honoris Causa" by the Technical University of Budapest. During his 35-year career in telecommunications he has held various research and academic posts in Hungary, Germany and the UK. Since 1986 he has been with the School of Electronics and Computer Science, University of Southampton, UK, where he holds the chair in telecommunications. He has successfully supervised 80 PhD students, co-authored 20 John Wiley/IEEE Press books on mobile radio communications totalling in excess of 10 000 pages, published 1300+ research entries at IEEE Xplore, acted both as TPC and General Chair of IEEE conferences, presented keynote lectures and has been awarded a number of distinctions. Currently he is directing a 100-strong academic research team, working on a range of research projects in the field of wireless multimedia communications sponsored by industry, the Engineering and Physical Sciences Research Council (EPSRC) UK, the European IST Programme and the Mobile Virtual Centre of Excellence (VCE), UK. He is an enthusiastic supporter of industrial and academic liaison and he offers a range of industrial courses. He is also a Governor of the IEEE VTS. During 2008 - 2012 he was the Editor-in-Chief of the IEEE Press and a Chaired Professor also at Tsinghua University, Beijing. His research is funded by the European Research Council's Senior Research Fellow Grant. For further information on research in progress and associated publications please refer to http://www-mobile.ecs.soton.ac.uk. He has 16000+ citations.